

# Mixed Convective Heat Transfer Flow of a Nanofluid through a Porous Medium in a Rectangular Cavity

D.R.V. Prasada Rao<sup>1</sup> G.N. Ramakrishna<sup>2</sup>

1. Department of Mathematics, S.K. University, Anantapur, India

2. Department of Mathematics, SSBN Degree & P.G. College, Anantapur, India

## Abstract

We consider Convective heat and mass transfer flow of a nanofluid through a porous medium in rectangular duct. The governing equations have been solved by using Galerkin finite element analysis with linear interpolation functions. The effects of nanoparticle volume fraction on all the flow characteristics have been discussed.

**Keywords:** Nanofluid, Rectangular Duct, Galerkin Method, Porous medium.

## 1. INTRODUCTION

Nanotechnology gives new chances to process and deliver materials with precious crystal sizes on the request of nanometres. Fluids with nanoparticles suspended in them are called nanofluid. Nanofluid can be characterized as designed colloids made of a base fluid and nanoparticles (1-100 nm). The term was introduced in 1995 by Choi of the Argonne National Laboratory; U.S.A. Contrasted and suspended routine particles of mille or micro meter measurements, nano fluids demonstrate better solidness; high thermal conductivity with irrelevant pressure drop. Successful utilizations of nanofluid would bolster the present trend toward segment scaling down by empowering the outline of littler but higher-power heat transfer systems.

The heat transfer upgrade utilizing nanofluids has been demonstrated by a large portion of the writings despite the fact that the expansion in heat expulsion rate fluctuates from study to contemplate. A 15% enhancement in Nusselt number Nu by utilizing CuO–water nanofluid with molecule volume convergence of  $\phi = 1\%$  has been accounted for by Behzadmehr et al., (3) while an increment of 4.57% with Reynolds number  $Re = 100$  has been accounted for by Apurba Kumar et al., (2). At the point when Re is increased from 100 to 1500, rate increment in Nu increased to 5.92%. They have recognized a most extreme of 34.83% increase in Nu by utilizing CuO–water nanofluid with  $\phi = 5\%$  and  $Re = 500$ . They have utilized homogeneous model for their study. While displaying the same nanofluid by two stage strategy expanded Nu from 34.83% to 67.76% with  $\phi = 5\%$  and  $Re = 500$ . This has been accounted for by Mohammed Kalteh et al., (10). They have additionally recognized an increase of 30% in heat transfer coefficient when particle diameter depicts from 100 nm to 30 nm. These outcomes demonstrate that displaying nanofluid as a solitary stage fluid lead to lower increment in heat transfer.

Oztop and Abu-Nanda (11) numerically examined the impact of various nanofluids on natural convection flow field and temperature disseminations in somewhat warmed rectangular walled in areas. The impact of utilizing nanofluids on heat transfer and fluid flow qualities in a rectangular shaped micro channel heat sink (MCHS) was numerically examined by Mohammed et al. (9). They communicated that the presence of nanoparticles could improve the cooling of the MCHS under compelling heat flux conditions with the ideal estimation of nanoparticles. Zeinali Heris et al., (14) have tentatively examined constrained convective heat transfer through square cross-sectional channel under laminar flow administration utilizing CuO/water nanofluid and this exploration is a part of an incorporated examination task to study heat transfer qualities through non-circular ducts and by using numerous sorts of nanoparticles. Zeinali Heris et al., (15) have researched constrained convective heat transfer attributes of three distinctive nanofluids (Al<sub>2</sub>O<sub>3</sub>/water, CuO/water and Cu/water) flowing through a square cross-segment channel in laminar flow under constant wall temperature boundary conditions. Krishnan et al., (8) have defined the transport equations considering nanofluid as a homogeneous fluid utilizing two - dimensional finite volume technique. By utilizing the defined conditions, the laminar flow attributes of various nanofluids through a rectangular channel are dissected. The nanofluid is a mixture of water as the base fluid and Al<sub>2</sub>O<sub>3</sub> and CuO as nanoparticles with various volume focuses and particle sizes. The variety of physical properties of base fluid is taken as temperature dependent. Ahmed H. Ali et al., (1) have explored the transient conduct of completely, laminar flow constrained convection with different groupings of nanoparticles and given Reynolds number on the heat transfer upgrade tentatively. Hejri et al., (6) have talked about laminar flow constrained convective heat transfer of Al<sub>2</sub>O<sub>3</sub>/water nanofluid intensive isosceles triangular cross sectional channel with steady divider heat flux was recreated numerically. Recreations were done in view of the single-stage model. The impacts of parameters, for example, nanoparticle focus, flow rate of nanofluids and the geometry of channels on warm conduct of nanofluids were contemplated. Zeinali Heris et al., (16) have considered the impacts of kind of the nanoparticles (Al<sub>2</sub>O<sub>3</sub>/CuO) and geometry (Square/Triangular pipe) on heat transfer are both researched at the same time, both square and triangular pipes are been with the same water powered width, and the recreation aftereffects of including diverse nanoparticles and distinctive geometry are concentrated all the more exhaustively. Additionally, the impact of nanoparticles sort on weight drop in conduits concentrated numerically,

and in light of the writing this subject is once in a while examined

Verschoor et al (13) have started the investigation of heat transfer through porous medium. Joseph et. al., (7) have considered laminar constrained convection in rectangular channels with unequal heat expansion on nearby sides. Teomann Ayhan et. al., (12) have considered heat transfer and flow structure in a rectangular channel with wing-sort Vortex Generator. Han-Chieh Chiu et. al., (5) have discussed about mixed convection heat transfer in horizontal rectangular ducts with radiation impacts. By utilizing Brinkman model Chittibabu et.al, (4) has discussed about convective flow in a porous rectangular duct with differentially heated side wall.

In this paper we investigate heat and mass transfer flow of CuO-Water Nanofluid and Al<sub>2</sub>O<sub>3</sub>-Water Nanofluids through porous medium in a rectangular duct. The effect of Nano particle Concentration on a temperature and concentration has been discussed at different horizontal and vertical levels.

## 2. PROBLEM FORMULATION

We consider the mixed convective heat and mass transfer flow of a viscous incompressible fluid in a saturated porous medium limited in the rectangular duct (Fig.1) whose base length is "a" and height "b". The heat flux on the base and top walls is maintained constant. The Cartesian coordinate system O (x, y) is picked with origin on the central axis of the duct and its base parallel to x-axis.

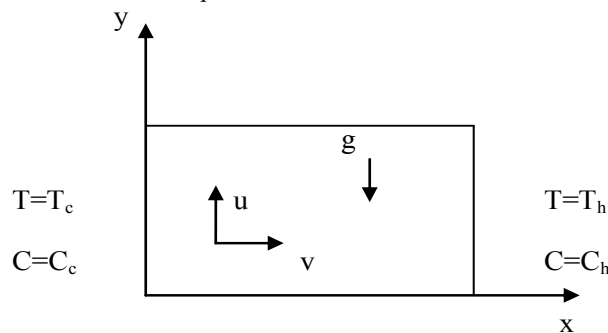


Fig. 1 SCHEMATIC DIAGRAMIC OF THE CONFIGURATION

Under the Boussinesq approximation the governing equations are given by

$$\frac{\partial u'}{\partial x'} + \frac{\partial v'}{\partial y'} = 0 \quad (1)$$

$$u' = -\frac{k}{\mu_{nf}} \left( \frac{\partial p'}{\partial x'} \right) \quad (2)$$

$$v' = -\frac{k}{\mu_{nf}} \left( \frac{\partial p'}{\partial y'} + \rho'_{nf} g \right) \quad (3)$$

$$(\rho c_p)_{nf} \left( u' \frac{\partial T'}{\partial x'} + v' \frac{\partial T'}{\partial y'} \right) = k_{nf} \left( \frac{\partial^2 T'}{\partial x'^2} + \frac{\partial^2 T'}{\partial y'^2} \right) \quad (4)$$

$$\left( u' \frac{\partial C}{\partial x'} + v' \frac{\partial C}{\partial y'} \right) = D_B \left( \frac{\partial^2 C}{\partial x'^2} + \frac{\partial^2 C}{\partial y'^2} \right) \quad (5)$$

where

$$T_0 = \frac{T_h + T_c}{2}, C_0 = \frac{C_h + C_c}{2} \quad (6)$$

where  $u'$  and  $v'$  are Darcy velocities along  $\theta(x, y)$  direction.  $T'$ ,  $C, p'$  and  $g'$  are the temperature, Concentration, pressure and acceleration due to gravity,  $T_c, C_c$  and  $T_h, C_h$  are the temperature and Concentration on the cold and warm side walls respectively.  $\rho', \mu_f, \nu_f$ , and  $\beta$  are the density, coefficients of viscosity, kinematic viscosity and thermal expansion of the fluid,  $k$  is the permeability of the porous medium,  $K_f$  is the thermal conductivity,  $C_p$  is the specific heat at constant pressure, and  $D_B$  is the molecular diffusivity.

The effective density of the nanofluid is given by

$$\rho_{nf} = (1 - \phi)\rho_f + \phi\rho_s \quad (7)$$

Where  $\phi$  is the solid volume fraction of nanoparticles  
 Thermal diffusivity of the nanofluid is

$$\alpha_{nf} = \frac{k_{nf}}{(\rho C_p)_{nf}} \quad (8)$$

Where the heat capacitance  $C_p$  of the nanofluid is obtained as

$$(\rho C_p)_{nf} = (1-\phi)(\rho C_p)_f + \phi(\rho C_p)_s \quad (9)$$

And the thermal conductivity of the nanofluid  $k_{nf}$  for spherical nanoparticles can be written as

$$\frac{k_{nf}}{k_f} = \frac{(k_s + 2k_f) - 2\phi(k_f - k_s)}{(k_s + 2k_f) + \phi(k_f - k_s)} \quad (10)$$

The thermal expansion coefficient of nanofluid can determine by

$$(\rho\beta)_{nf} = (1-\phi)(\rho\beta)_f + \phi(\rho\beta)_s \quad (11)$$

Also the effective dynamic viscosity of the nanofluid given by

$$\mu_{nf} = \frac{\mu_f}{(1-\phi)^{2.5}}, \quad (12)$$

Where the subscripts nf, f and s represent the thermo physical properties of the nanofluid, base fluid and the nanosolid particles respectively and  $\phi$  is the solid volume fraction of the nanoparticles. The thermo physical properties of the nanofluid are given in Table 1 (See Oztop and Abu-Nada (27)).

Table 1

Physical properties	Fluid phase	CuO(Copper)	Al <sub>2</sub> O <sub>3</sub> (Alumina)	TiO <sub>2</sub> (Titanium dioxide)
C <sub>p</sub> (j/kg K)	4179	385	765	686.2
P(kg m <sup>3</sup> )	997.1	8933	3970	4250
k(W/m K)	0.613	400	40	8.9538
σ(S/m)	5.5x10 <sup>-6</sup>	59.5x10 <sup>6</sup>	35x10 <sup>6</sup>	2.6 x10 <sup>6</sup>

The boundary conditions are

$$\begin{aligned} u' = v' = 0 & \quad \text{on the boundary of the duct} \\ T' = T_c, C=C_c & \quad \text{on the side wall to the left} \\ T' = T_h, C=C_h & \quad \text{on the side wall to the right} \\ \frac{\partial T'}{\partial y} = 0, \frac{\partial C}{\partial y} = 0 & \quad \text{on the top (y = 0) and bottom} \end{aligned} \quad (13)$$

$$u = v = 0 \quad \text{Walls(y = 0) which are insulated.}$$

We now introduce the following non-dimensional variables

$$\begin{aligned} x' = ax; \quad y' = by; \quad h = b/a \\ u' = \left(\frac{v_f}{a}\right)u; \quad v' = \left(\frac{v_f}{a}\right)v; \quad p' = \left(\frac{v_f^2 \rho}{a^2}\right)p \\ T' = T_0 + \theta (T_h - T_c); \quad C' = C_0 + C (T_h - T_c) \end{aligned} \quad (14)$$

$$\begin{aligned} A_1 = \frac{1}{(1-\phi)^{2.5}}, \quad A_2 = (1-\phi) + \phi\left(\frac{\rho_s}{\rho_f}\right), \\ A_3 = 1 - \phi + \phi\left(\frac{(\rho C_p)_s}{(\rho C_p)_f}\right), \quad A_4 = 1 - \phi + \phi\left(\frac{(\rho\beta)_s}{(\rho\beta)_f}\right), \quad A_5 = \frac{k_{nf}}{k_f} \end{aligned}$$

In view of the equation of continuity we introduce the stream function  $\psi$  as

$$u = \frac{\partial \psi}{\partial y}; \quad v = -\frac{\partial \psi}{\partial x}$$

the governing equations in the non-dimensional form after eliminating the pressure(p)are

$$D^{-1} \left( \frac{\partial^2 \psi^k}{\partial x^2} + \frac{\partial^2 \psi^k}{\partial y^2} \right) = -GA_1 A_4 \left( \frac{\partial \theta^k}{\partial x} \right) \quad (15)$$

$$\left( \frac{\partial^2 \theta^k}{\partial x^2} + \frac{\partial^2 \theta^k}{\partial y^2} - \text{Pr} A_3 \left( \frac{\partial \psi^k}{\partial y} \frac{\partial \theta^k}{\partial x} - \frac{\partial \psi^k}{\partial x} \frac{\partial \theta^k}{\partial y} \right) \right) = 0 \quad (16)$$

$$\frac{\partial^2 C^k}{\partial x^2} + \frac{\partial^2 C^k}{\partial y^2} - \text{Sc} \left( \frac{\partial \psi^k}{\partial y} \frac{\partial C^k}{\partial x} - \frac{\partial \psi^k}{\partial x} \frac{\partial C^k}{\partial y} \right) = 0 \quad (17)$$

Where

$$G = \frac{g\beta(T_h - T_c)a^3}{\nu^2} \quad (\text{Grashof number}) \quad \text{Pr} = \frac{mC_p}{k_f} \quad (\text{Prandtl number}), \quad D^{-1} = \frac{a^2}{k} \quad (\text{Inverse Darcy Parameter})$$

$$\text{Sc} = \frac{\nu}{D_B} \quad (\text{Schmidt number})$$

The 4 boundary conditions are

$$\frac{\partial \psi}{\partial x} = 0, \quad \frac{\partial \psi}{\partial y} = 0 \quad \text{on} \quad x = 0 \quad \& \quad 1 \quad (18)$$

$$\theta = 1 \quad c = 1 \quad \text{on} \quad x = 0$$

$$\theta = 0 \quad c = 0 \quad \text{on} \quad x = 1 \quad (19)$$

### 3. FINITE ELEMENT ANALYSIS AND SOLUTION OF THE PROBLEM:

The Galerkin finite element analysis is carried out with linear polynomial approximation functions. For different variations in governing parameters, the behavior of temperature and concentration profiles are discussed. The global coupled matrices for the velocity, temperature and concentration are obtained.

Assuming an arbitrary element  $e^k$  and let  $u^k$ ,  $\theta^k$  and  $C^k$  be the values of  $u$ ,  $\theta$  and  $C$  in the element  $e^k$ , the error residuals are defined as

$$E_\theta^i = \left( \frac{\partial^2 \theta^k}{\partial x^2} + \frac{\partial^2 \theta^k}{\partial y^2} - \text{Pr} A_3 \left( \frac{\partial \psi^k}{\partial y} \frac{\partial \theta^k}{\partial x} - \frac{\partial \psi^k}{\partial x} \frac{\partial \theta^k}{\partial y} \right) \right)$$

$$E_c^i = \frac{\partial^2 C^k}{\partial x^2} + \frac{\partial^2 C^k}{\partial y^2} - \text{Sc} \left( \frac{\partial \psi^k}{\partial y} \frac{\partial C^k}{\partial x} - \frac{\partial \psi^k}{\partial x} \frac{\partial C^k}{\partial y} \right)$$

$$E_\psi^i = D^{-1} \left( \frac{\partial^2 \psi^k}{\partial x^2} + \frac{\partial^2 \psi^k}{\partial y^2} \right) + GA_1 A_4 \left( \frac{\partial \theta^k}{\partial x} \right)$$

These are expressed as linear combinations in terms of respective local nodal values.

$$\psi^k = N_1^k \psi_1^k + N_2^k \psi_2^k + N_3^k \psi_3^k \quad (20a)$$

$$\theta^k = N_1^k \theta_1^k + N_2^k \theta_2^k + N_3^k \theta_3^k \quad (20b)$$

$$C^k = N_1^k C_1^k + N_2^k C_2^k + N_3^k C_3^k \quad (20c)$$

Where  $\psi_1^k$ ,  $\psi_2^k$ ,  $\psi_3^k$  are Lagrange's linear polynomials.

Galerkin's method is used to convert the partial differential Eqs. (15) – (17) into matrix form of equations which results into 3x3 local stiffness matrices. All these local matrices are assembled in a global matrix by substituting the global nodal values of order I.

In the problem under consideration, for computational purpose, we choose uniform mesh of 10 triangular elements (Fig. 2). The domain has vertices whose global coordinates are (0,0), (1,0) and (1,c) in the non-dimensional form. Let  $e_1, e_2, \dots, e_{10}$  be the ten elements and let  $\theta_1, \theta_2, \dots, \theta_{10}$  be the global values of  $\theta$  and  $\psi_1, \psi_2, \dots, \psi_{10}$  be the global values of  $\psi$  at the ten global nodes of the domain (Fig. 2).

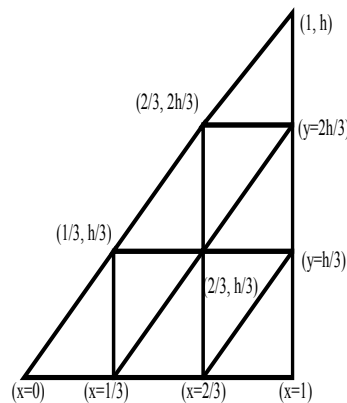


Fig. 2 SCHEMATIC DIAGRAM OF THE CONFIGURATION

The global matrix equation for  $\theta$  is

$$A_3 X_3 = B_3 \quad (21)$$

The global matrix equation for C is

$$A_4 X_4 = B_4 \quad (22)$$

The global matrix equation for  $\psi$  is

$$A_5 X_5 = B_5 \quad (23)$$

Where  $A_3, A_4, A_5$  are Global Square stiffness Matrices and  $B_3, B_4, B_5$  are Column matrices involving the governing parameters

The global matrix equations are coupled and are solved under the following iterative procedures. At the beginning of the first iteration the values of  $(\psi_i)$  are taken to be zero and the global equations (16) & (17) are solved for the nodal values of  $\theta$  and C. These nodal values  $(\theta_i)$  and  $(C_i)$  obtained are then used to solve the global equation (15) to obtain  $(\psi_i)$ . In the second iteration these  $(\psi_i)$  values are obtained are used in (16) & (17) to calculate  $(\theta_i)$  and  $(C_i)$  and vice versa. The three equations are thus solved under iteration process until two consecutive iterations differ by a reassigned percentage.

The dimensionless Nusselt numbers (Nu) and Sherwood Numbers (Sh) on the non-insulated boundary wall of the rectangular duct are calculated using the formula

$$Nu = \left( \frac{\partial \theta}{\partial x} \right)_{x=1} \text{ and } Sh = \left( \frac{\partial C}{\partial x} \right)_{x=1}$$

Nusselt Number & Sherwood number on the side wall  $x=1$  in different regions are given by

$$Nu_1 = \binom{n}{5.1}_x \theta_3 + \binom{n}{5.2}_x \theta_4 + \binom{n}{5.3}_x \theta_5, \quad Sh_1 = \binom{n}{5.1}_x C_3 + \binom{n}{5.2}_x C_4 + \binom{n}{5.3}_x C_5, \quad (0 \leq y \leq h/3)$$

$$Nu_2 = \binom{n}{6.1}_x \theta_6 + \binom{n}{6.2}_x \theta_5 + \binom{n}{6.3}_x \theta_9, \quad Sh_2 = \binom{n}{6.1}_x C_6 + \binom{n}{6.2}_x C_5 + \binom{n}{6.3}_x C_9, \quad (h/3 \leq y \leq 2h/3)$$

$$Nu_3 = \binom{n}{9.1}_x \theta_8 + \binom{n}{9.2}_x \theta_9 + \binom{n}{9.3}_x \theta_{10}, \quad Sh_3 = \binom{n}{9.1}_x C_8 + \binom{n}{9.2}_x C_9 + \binom{n}{9.3}_x C_{10}, \quad (2h/3 \leq y \leq h)$$

and the corresponding expressions are

$$Nu_1 = 3 - 3\theta_3, \quad Sh_1 = 3 - 3C_3 \quad (0 \leq y \leq h/3), \quad Nu_2 = 3 - 3\theta_5, \quad Sh_2 = 3 - 3C_5 \quad (h/3 \leq y \leq 2h/3)$$

$$Nu_3 = 3 - 3\theta_7, \quad Sh_3 = 3 - 3C_7 \quad (2h/3 \leq y \leq h)$$

#### 4. RESULTS AND DISCUSSION:

In this analysis we investigate the effect of nanoparticles concentration on on temperature and concentration at different levels in a rectangular duct. The analysis has been carried out for two different types of CuO-water and  $Al_2O_3$ -water nanofluids. Figs.3-6 represent the variation of temperature with nano particle volume fraction ( $\phi$ ).

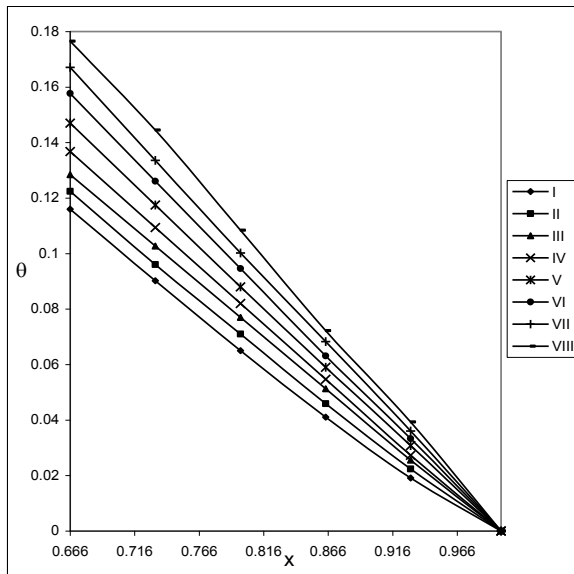


Fig.3 Variation of  $\theta$  with  $\phi$  at  $y = 2h/3$   
 CuO-water Al<sub>2</sub>O<sub>3</sub>-water  
 I II III IV V VI VII VIII  
 $\phi$  0.1 0.3 0.5 0.7 0.1 0.3 0.5 0.7

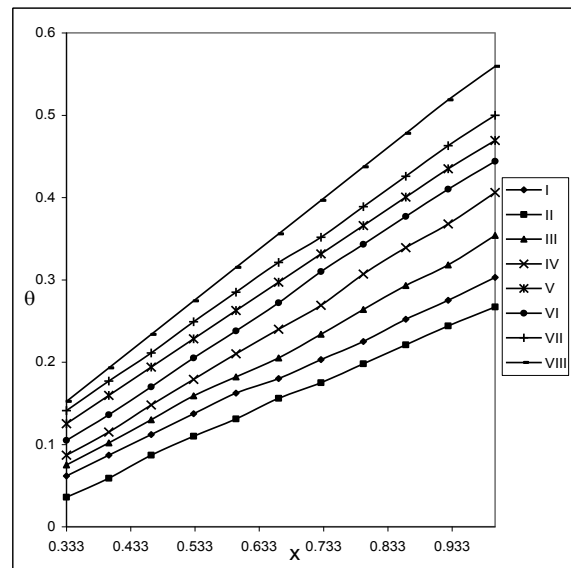


Fig.4 Variation of  $\theta$  with  $\phi$  at  $y = h/3$   
 CuO-water Al<sub>2</sub>O<sub>3</sub>-water  
 I II III IV V VI VII VIII  
 $\phi$  0.1 0.3 0.5 0.7 0.1 0.3 0.5 0.7

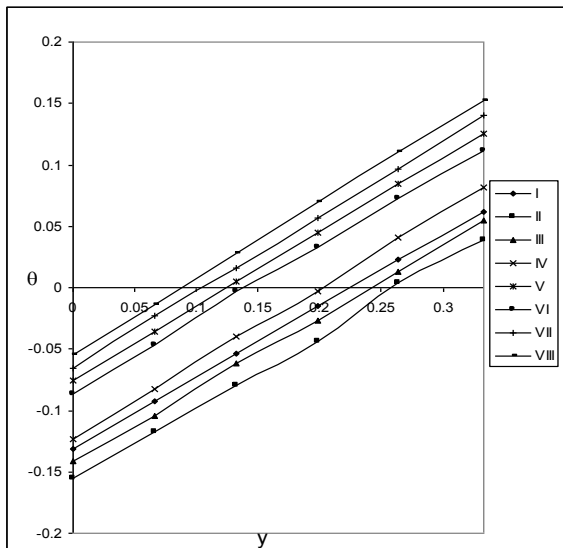


Fig.5 Variation of  $\theta$  with  $\phi$  at  $x = 1/3$   
 CuO-water Al<sub>2</sub>O<sub>3</sub>-water  
 I II III IV V VI VII VIII  
 $\phi$  0.1 0.3 0.5 0.7 0.1 0.3 0.5 0.7

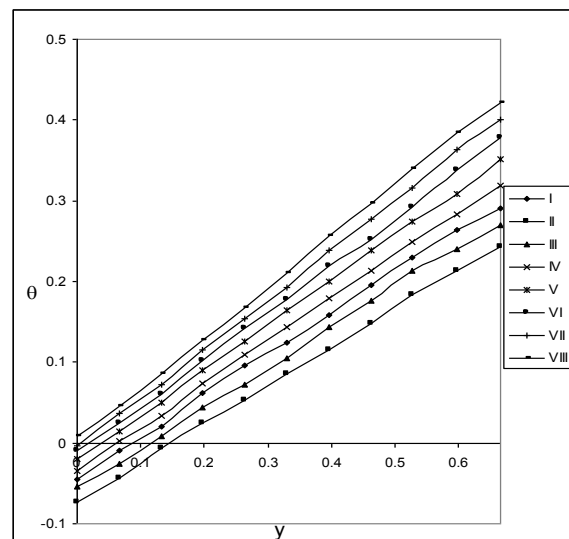


Fig.6 Variation of  $\theta$  with  $\phi$  at  $x = 2/3$   
 CuO-water Al<sub>2</sub>O<sub>3</sub>-water  
 I II III IV V VI VII VIII  
 $\phi$  0.1 0.3 0.5 0.7 0.1 0.3 0.5 0.7

An increase in  $\phi$  enhances the actual temperature at  $y = \frac{2h}{3}$  and reduces at  $y = \frac{h}{3}$ ,  $x = \frac{1}{3}$  and  $x = \frac{2}{3}$  levels for both types of nanofluid. The volume fraction parameter  $\phi$  is found to be of significance in this problem, which has non negligible effect on the improvement of the heat characteristics of the fluid. Also the values of actual temperature in CuO-water nanofluid are relatively smaller than those values of actual temperature in Al<sub>2</sub>O<sub>3</sub>-water nanofluid.

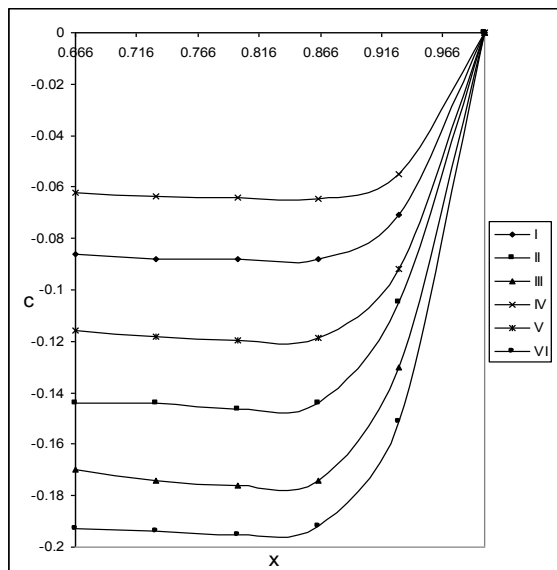


Fig.7 Variation of C with  $\phi$  at  $y=2h/3$   
 CuO-water  $\text{Al}_2\text{O}_3$ -water  
 I II III IV V VI  
 $\phi$  0.1 0.3 0.5 0.1 0.3 0.5

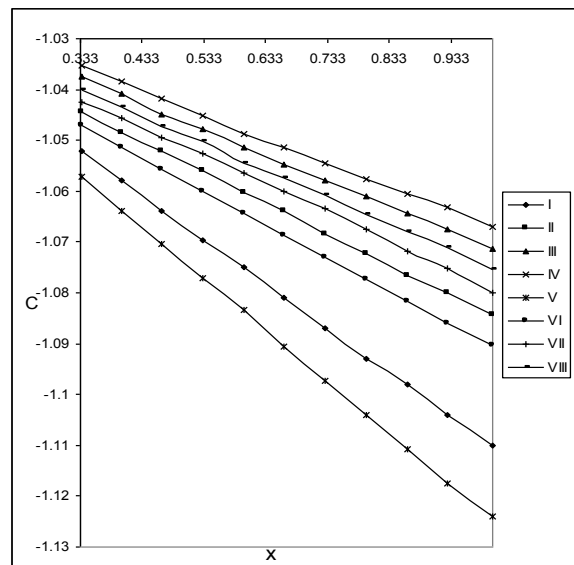


Fig.8 Variation of C with  $\phi$  at  $y=h/3$   
 CuO-water  $\text{Al}_2\text{O}_3$ -water  
 I II III IV V VI VII VIII  
 $\phi$  0.1 0.3 0.5 0.7 0.1 0.3 0.5 0.7

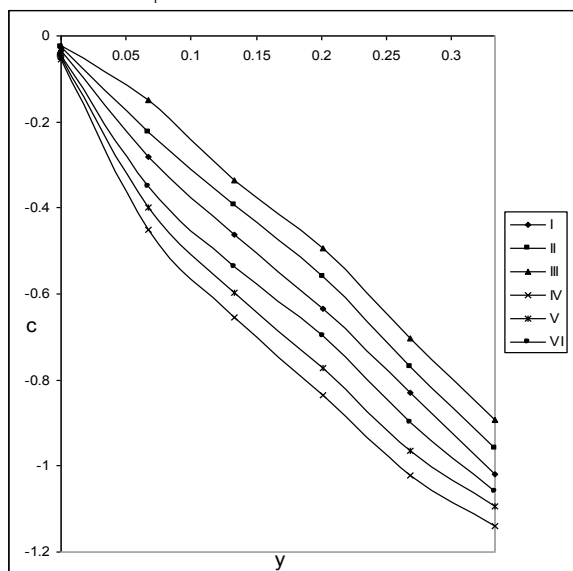


Fig.9 Variation of C with  $\phi$  at  $x=1/3$   
 CuO-water  $\text{Al}_2\text{O}_3$ -water  
 I II III IV V VI  
 $\phi$  0.1 0.3 0.5 0.1 0.3 0.5

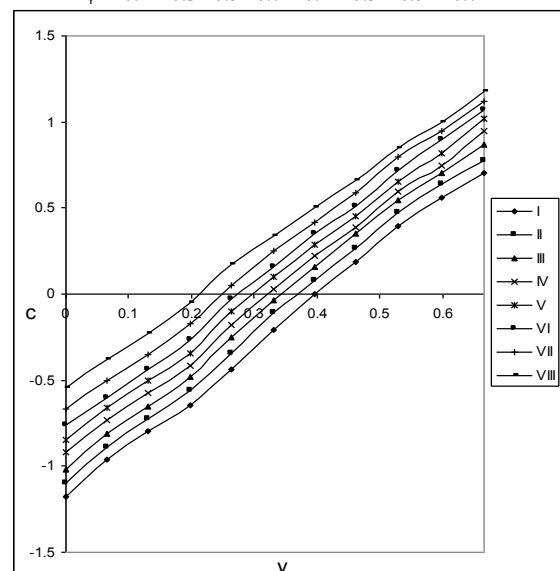


Fig.10 Variation of C with  $\phi$  at  $x=2/3$   
 CuO-water  $\text{Al}_2\text{O}_3$ -water  
 I II III IV V VI VII VIII  
 $\phi$  0.1 0.3 0.5 0.7 0.1 0.3 0.5 0.7

It can be seen from these figures that an increase in the nano particle volume fraction  $\phi$  enhances the nano particle fraction concentration at all vertical and horizontal levels fixing the other parameters. It is found that at  $y=\frac{2h}{3}$  and  $x=\frac{2}{3}$  levels, the actual concentration in CuO-water nanofluid is relatively greater than those values in  $\text{Al}_2\text{O}_3$ -water nanofluid. At  $y=\frac{h}{3}$  and  $x=\frac{1}{3}$  levels the actual concentration in CuO-water nanofluid are relatively lesser than those values in  $\text{Al}_2\text{O}_3$ -water nanofluid.

**Effect of parameter on Nusselt number and Sherwood number:**

The rate of heat transfer (Nusselt Number) is shown in the Table-2 for different values of  $\phi$ . The variation of Nu with volume fraction parameter  $\phi$  shows that the Nusselt number on all quadrants enhances in CuO-water nanofluid and reduces in  $\text{Al}_2\text{O}_3$ -water nano fluid. The values of Nusselt number in CuO-water nanofluid are relatively larger than those in  $\text{Al}_2\text{O}_3$ -water nanofluid.

TABLE – 2  
 Nusselt Number (Nu)

		CuO-water			Al <sub>2</sub> O <sub>3</sub> -water		
		Nu1	Nu2	Nu3	Nu1	Nu2	Nu3
φ	0.1	2.5678	2.5897	2.6045	2.4897	2.3912	2.3315
	0.3	2.6067	2.6167	2.6338	2.4765	2.3440	2.3112
	0.7	2.6206	2.6312	2.6798	2.4532	2.3123	2.3076

The local rate of mass transfer (Sherwood number) is shown in the Table-3 for φ. An increase in the volume fraction parameter φ reduces the Sherwood number on all the quadrants reduce in both types of nanofluids. Also it is found that the values of Sherwood number reduces as move from the lower to middle quadrant and it increases on the upper quadrant in both types of nanofluids. In all the above variations we find that the values of the Sherwood number on all the three quadrants in CuO-water nanofluid are relatively lesser than those values in Al<sub>2</sub>O<sub>3</sub>-water nanofluid.

TABLE – 3  
 Sherwood Number (Sh)

		Cu-water			Al <sub>2</sub> O <sub>3</sub> -water		
		Sh1	Sh2	Sh3	Sh1	Sh2	Sh3
φ	0.1	3.6548	2.9987	3.9976	4.5678	3.6578	4.6789
	0.3	3.4536	2.8765	4.0123	4.3456	3.5546	4.8909
	0.7	3.3876	2.6547	4.4567	3.9986	3.4467	4.9534

- An increase in nano particle volume fraction φ enhances the actual temperature at  $y = \frac{2h}{3}$  and reduces at  $y = \frac{h}{3}$ ,  $x = \frac{1}{3}$  and  $x = \frac{2}{3}$  levels for both types of nanofluid. The volume fraction parameter φ is found to be of significance in this problem, which has non negligible effect on the improvement of the heat characteristics of the fluid. Also the values of actual temperature in CuO-water nanofluid are relatively smaller than those values of actual temperature in Al<sub>2</sub>O<sub>3</sub>-water nanofluid.
- An increase in the nano particle volume fraction φ enhances the nano particle fraction concentration at all vertical and horizontal levels fixing the other parameters. It is found that at  $y = \frac{2h}{3}$  and  $x = \frac{2}{3}$  levels, the actual concentration in CuO-water nanofluid is relatively greater than those values in Al<sub>2</sub>O<sub>3</sub>-water nanofluid. At  $y = \frac{h}{3}$  and  $x = \frac{1}{3}$  levels the actual concentration in CuO-water nanofluid are relatively lesser than those values in Al<sub>2</sub>O<sub>3</sub>-water nanofluid.

The Nusselt number on all the quadrants enhances in CuO-water nanofluid and reduces in Al<sub>2</sub>O<sub>3</sub>-water nano fluid with increase in φ.

The Sherwood number on all the three quadrants decreases on lower and middle quadrants and enhances on the upper quadrant with increasing φ in both types of nanofluid.

## 5. REFERENCES

1. Ahmed H. Ali, Tahseen A.Al-Hattab, Experimental study of transient forced convection heat transfer nanofluid in triangular duct, IJIRSET, V.3, Issue 8, pp. 15703-15715, (2014).
2. Apurba Kumar Santra, Swarnendu Sen, Niladri Chakraborty., Study of heat transfer due to laminar flow of copper–water nanofluid through two isothermally heated parallel plates, International Journal of Thermal Sciences, V.48, pp.391–400, (2009).
3. Behzadmehr, A., Saffar-Avval, M., Galanis, N., Prediction of turbulent forced convection of a nanofluid in a tube with uniform heat flux using a two phase approach, International Journal of Heat and Fluid Flow, V.28, pp.211-219, (2007).
4. Chittibabu. D., Prasada Rao. D.R.V., Krishna D.V.: Convection flow through a porous medium in ducts. Act science Indica V. 30 2M, pp. 635-642 (2006).
5. Han–Chien Chiu, Jer-Huan Jang, Wei-Monyan: Mixed convection heat transfer in Horizontal rectangular ducts with radiation effects. Int. Journal of Heat Mass transfer V.50, pp.2874-2882, (2007).
6. Hejri M, Hojjat M, Nano fluids flow and heat transfer through Isosceles Triangular Channel: Numerical Simulation, International Conference on Heat Transfer and Fluid Flow, P. 211, (2014).
7. Joseph, J. Savino and Robert Siegel: Laminar forced convection in Rectangular channels with unequal Heat addition on adjacent sides. Int. J. Heat Mass transfer V. 71, pp.733-741 (1964).
8. Krishnan K.N, Aboobacker Kadangel, Fluid Dynamics Characteristics of Nanofluids in Rectangular Duct,

- International Journal of Scientific & Engineering Research, V. 5, Issue 10, (2014).
9. Mohammed HA, Gunnasegarana P, Shuaiba NH Heat transfer in rectangular microchannels heat sink using nanofluids. *Int. Commun. Heat and Mass Transfer* V.37, pp.14961503 (2010).
  10. Mohammed Kalteh, Abbassi, A., Saffar-Avval, M., Harting, J., Eulerian – Eulerian two-phase numerical simulation of nanofluid laminar forced convection in a micro channel, *International Journal of Heat and Fluid Flow* V.32, pp.107-116, (2011).
  11. Oztop HF, Abu-Nada E Numerical study of natural convection in partially heated rectangular enclosures filled with nanofluids. *Int. J. Heat Fluid Flow* V.29 pp.1326-1336 (2008).
  12. Teoman Ayhan, Hayati Olgum : Betul Ayhan : Heat transfer and flow structure in a Rectangular channel with wing -1. type vortex Generator. *Tr. J. of Engineering and Environmental Science* , V.22 , pp.185-195(1998).
  13. Verschoor, J.D, and Greebler, P : Heat Transfer by gas conduction and radiation in fibrous insulation *Trans. Am. Soc. Mech. Engrs.*, PP. 961-968 (1952).
  14. Zeinali Heris S, Taofik H, Nassan, S.H, Noie, CuO/water Nanofluid convective Heat Transfer through Square Duct Under Uniform Heat Flux, V. 7, No. 3, pp. 111-120 (2011).
  15. Zeinali Heris S, Kazemi-Beydokhti A, Noie S.H and Rezvan S, Numerical study on convective heat transfer of Al<sub>2</sub>O<sub>3</sub>/water, CuO/water and Cu/water nanofluids through square cross-section duct in laminar flow, *Engineering Applications of Computational Fluid Mechanics* V.6, No.1, pp.1-14 (2012).
  16. Zeinali Heris S, Oghazian F, Khademi M, Saeedi E, Simulation of Convective Heat Transfer and Pressure Drop in Laminar Flow of Al<sub>2</sub>O<sub>3</sub>/water and CuO/water Nanofluids Through Square and Triangular Cross-Sectional Ducts, *Journal of Renewable Energy and Environment*, V.2, No.1, 6-18 (2015).